Reflection absorption infrared spectroscopy and temperature programmed desorption investigations of the interaction of methanol with a graphite surface

A. S. Bolina, A. J. Wolff, and W. A. Brown[a]
Department of Chemistry, University College London, 20 Gordon Street, London WC1H 0AJ, United Kingdom

Reflection absorption infrared spectroscopy (RAIRS) and temperature programmed desorption (TPD) have been used to investigate the adsorption of methanol (CH_3OH) on the highly oriented pyrolytic graphite (HOPG) surface. RAIRS shows that CH_3OH is physisorbed at all exposures and that crystalline CH_3OH can be formed, provided that the surface temperature and coverage are high enough. It is not possible to distinguish CH_3OH that is closely associated with the HOPG surface from CH_3OH adsorbed in multilayers using RAIRS. In contrast, TPD data show three peaks for the desorption of CH_3OH. Initial adsorption leads to the observation of a peak assigned to the desorption of a monolayer. Subsequent adsorption leads to the formation of multilayers on the surface and two TPD peaks are observed which can be assigned to the desorption of multilayer CH_3OH. The first of these shows a fractional order desorption, assigned to the presence of hydrogen bonding in the overlayer. The higher temperature multilayer desorption peak is only observed following very high exposures of CH_3OH to the surface and can be assigned to the desorption of crystalline CH_3OH. © *2005 American Institute of Physics.* [DOI: 10.1063/1.1839554]

I. INTRODUCTION

Methanol (CH_3OH) is found in the interstellar medium (ISM) in the form of interstellar ices, frozen out on the surface of dust grains.[1] It is widely thought that the majority of the CH_3OH present in these ices does not form in the gas phase and subsequently accrete on the surface of the grains. Instead it is hypothesized that CH_3OH forms directly on the surface of the dust, as a result of the successive heterogeneous hydrogenation of CO.[2,3] With this in mind, we have used reflection absorption infrared spectroscopy (RAIRS) and temperature programmed desorption (TPD) to investigate the adsorption of CH_3OH on, and its desorption from, a highly oriented pyrolytic graphite (HOPG) surface held at around 100 K. This investigation forms part of a wider study of the mechanism of formation of CH_3OH on dust grain analog surfaces.

Dust grains in the ISM are thought to consist mainly of carbonaceous and silicaceous material and are often covered in films of ice.[1] HOPG, and other carbon based surfaces, can be considered suitable analogs of dust grains and have been used previously in investigations of H_2 formation on dust grains.[4–7] The temperature in the ISM, where these ice covered grains are found, is around 10–20 K. Although the experiments described here are not undertaken at this temperature, they still allow an understanding of the interaction of CH_3OH with the HOPG surface to be gained.

The only previous investigation of CH_3OH adsorption on HOPG was performed by Wang *et al.*[8] using atomic force microscopy. This study showed physisorbed multilayer growth of CH_3OH on HOPG. Irregular islands of CH_3OH were observed and it was possible to distinguish between CH_3OH adsorbed in a bilayer and in a multilayer.

In contrast, the interaction of CH_3OH with metal surfaces has been widely studied due to its widespread application in elementary catalytic processes[9] and in fuel cells.[10,11] The adsorption and reaction of CH_3OH with metal surfaces have been discussed in several review articles.[12–14] CH_3OH has been shown to decompose to form methoxy (H_3CO-) on most metal surfaces[12,15–29] and the decomposition can be promoted by coadsorbed oxygen, particularly on Au, Ag, and Cu surfaces.[20,21,27,30,31] At lower temperatures, physisorbed multilayers of CH_3OH are observed, adsorbed on top of the underlying chemisorbed layer.[15–17,19,21–25,27,29,32–35]

A detailed RAIRS and TPD study of the adsorption of CH_3OH on Pd{110} at 124 K was performed by Pratt and co-workers.[15] Initial adsorption of CH_3OH led to the formation of a chemisorbed layer. Further adsorption then led to the formation of a multilayer. RAIRS was used to show that the multilayer consisted of a crystalline structure in which hydrogen bonded chains of molecules were formed.[15] In addition to the crystalline multilayer, a "sandwich" layer was also identified on Pd{110}[15] which had a different RAIR spectrum to both the multilayer and the chemisorbed monolayer. The formation of crystalline multilayers has also been observed for CH_3OH adsorbed on Ru{001},[25] polycrystalline Pt,[32] Pt{111},[34] Rh{100},[28] Pd{100},[22] and Cu{110}.[35] In all cases, formation of the crystalline phase was temperature dependant and could only be observed following a certain minimum exposure of CH_3OH. The formation of a crys-

[a]Author to whom correspondence should be addressed. Fax: + 44 20 7679 7463. Electronic mail: w.a.brown@ucl.ac.uk

talline multilayer was characterized by the observation of splitting in the O–H region of the infrared spectrum, with bands being observed at 3301 and 3193 cm^{-1}.[15,34]

TPD studies of the desorption of CH_3OH from a range of metal surfaces have also been performed. Pratt and co-workers[15] observed two main peaks in the TPD spectrum for CH_3OH adsorbed on Pd{110} at 143 and 230 K. The lower temperature peak did not saturate and was assigned to physisorbed CH_3OH, while the higher temperature peak was assigned to the desorption of chemisorbed CH_3OH.[15] This TPD spectrum was in broad agreement with those observed for CH_3OH desorption from other metal surfaces.[22,25,28,32,35] However, a TPD study of CH_3OH desorption from Ag{111} showed three desorption features.[33] The highest temperature peak was assigned to the desorption of the monolayer. The two lower temperature peaks were assigned to the desorption of the multilayer, with the higher of the two peaks being assigned to amorphous CH_3OH desorption and the lower of the two peaks assigned to the desorption of crystalline CH_3OH.[33] This is in disagreement with the TPD data for desorption of CH_3OH from Pd{110}, where Pratt, Escott, and King[15] indicate that they could not distinguish the crystalline and amorphous CH_3OH phases during desorption.

Several authors[22,36] have noted that multilayer desorption peaks, observed in the TPD for increasing exposures of CH_3OH to the surface, do not share a leading edge as would be expected for zero order desorption. This suggests that multilayer desorption is fractional order, and has previously been attributed to the formation of hydrogen bonds in the physisorbed layer.[22,36] Further evidence for the strong influence of hydrogen bonding on CH_3OH adsorption comes from the observation that occupation of the multilayer is often observed even before the monolayer is saturated.[15,28,36]

Here we describe detailed RAIRS and TPD investigations of the adsorption of CH_3OH on HOPG at both 100 and 130 K. The latter temperature was chosen as it is close to the temperature at which the amorphous to crystalline transition is observed for solid CH_3OH.[34]

II. METHODOLOGY

Experiments were performed in an ultrahigh vacuum (UHV) chamber that has a base pressure of $\leq 2 \times 10^{-10}$ mbar. The HOPG sample was purchased from Goodfellows Ltd. and was cleaved prior to installation in the UHV chamber using the "Scotch tape" method. The sample was cleaned before each experiment by annealing at 500 K in UHV for 3 min. Sample cleanliness was confirmed by the absence of any desorbing species during TPD experiments performed with no dosage. The sample was cooled to ~ 100 K by pouring liquid nitrogen down the cold finger on which the sample was mounted. CH_3OH (99.9% purity, BDH Laboratory Supplies Ltd.) was admitted into the chamber by means of a high precision leak valve and the purity was checked with a quadrupole mass spectrometer before each experiment. All exposures are measured in Langmuir (L), where 1 L$= 10^{-6}$ mbar s.

RAIR spectra were recorded using a Mattson instruments RS1 research series Fourier transform infrared spectrometer coupled to a liquid nitrogen cooled mercury cad-
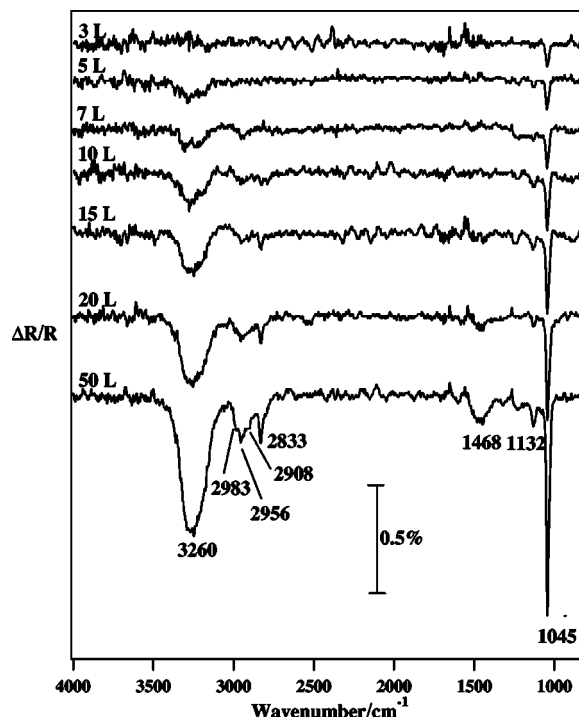

FIG. 1. RAIR spectra recorded following the adsorption of CH_3OH on HOPG at 97 K. The given exposures are marked on the figure.

mium telluride (MCT) detector. All spectra were taken at a resolution of 4 cm^{-1} and are the result of the coaddition of 256 scans, taking ≈ 3 min to collect each spectrum. In RAIRS experiments where the sample was heated, it was annealed to a predetermined temperature, held at this temperature for 3 min, and then cooled back down to the base temperature before a spectrum was recorded. TPD spectra were recorded with a Hiden Analytical HAL201 quadrupole mass spectrometer. All spectra were recorded at a heating rate of 0.5 K s^{-1}.

III. RESULTS AND DISCUSSION

A. RAIRS experiments

RAIR spectra recorded following CH_3OH adsorption on HOPG at 97 K are shown in Fig. 1. Initial exposure of the surface to CH_3OH leads to the appearance of one band at 1045 cm^{-1}. With increasing exposure, this band increases in intensity, but does not shift in frequency. Following a 5 L exposure of CH_3OH a broad band, centered at 3260 cm^{-1}, also grows into the spectrum. Similar to the band at 1045 cm^{-1}, this band grows in intensity with increasing exposure but does not undergo a frequency shift. As the CH_3OH exposure is increased to 7 L and above, additional bands at 1132, 1468, 2833, 2908, 2956, and 2983 cm^{-1} also grow into the spectra seen in Fig. 1. Increasing the exposure further (up to a total of 300 L) increases the intensity of these bands but does not lead to the observation of any additional spectral features. It is not possible to saturate any of these bands with increasing exposure, indicating that they are due to the formation of physisorbed multilayers of CH_3OH on the HOPG surface.

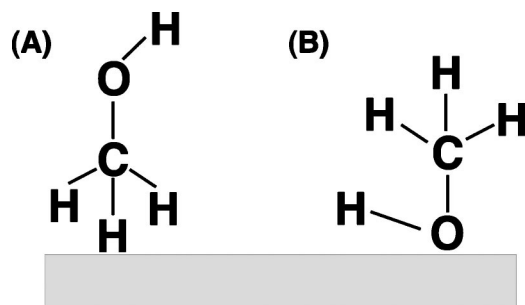FIG. 2. Possible orientations of CH_3OH adsorbed on HOPG in the mono-layer regime. The most likely orientation is that shown in (b) where the O atom of the CH_3OH bonds closest to the surface.

It is clear from the spectra in Fig. 1 that chemisorbed CH_3OH is not formed on HOPG. However, at lower exposures (≤ 7 L) it is assumed that the CH_3OH is adsorbed on the HOPG surface in a monolayer, although it is not possible to distinguish between monolayer and multilayer adsorption in the RAIR spectra. TPD spectra (shown later) do show a clear difference between first layer (monolayer) CH_3OH and subsequent multilayer CH_3OH. The bands observed in the RAIR spectrum of the monolayer, at 1045 and 3260 cm^{-1}, can be assigned by comparison with previous data for CH_3OH adsorbed on metal surfaces[15–17,19,21–25,27,29,32–35] and in an Ar matrix.[37] The bands are assigned to the symmetric C–O stretch and symmetric O–H stretch of CH_3OH, respectively. Since these bands are not shifted, compared to those

seen for higher exposures of CH_3OH (Fig. 1), it is assumed that the monolayer is physisorbed on the HOPG surface.

The data shown in Fig. 1 for low exposures give an indication of the orientation of the first few layers of CH_3OH adsorbed on the HOPG surface. The selection rules imposed by RAIRS on a metal surface also hold for adsorption on HOPG[38] and state that only vibrational modes with a component of the dipole moment perpendicular to the surface can be observed. Figure 1 shows that, at low exposures, only the C–O stretch of CH_3OH is observed, suggesting that the O–H stretch is lying parallel to the surface as shown in Fig. 2. It is most likely that CH_3OH bonds to the surface via its O atom as shown in Fig. 2(b), in agreement with previous observations on other surfaces.[36]

As already discussed, higher exposures of CH_3OH on HOPG lead to the formation of multilayers on the surface, and the bands observed in the RAIR spectra in Fig. 1 are in good agreement with those observed for multilayer CH_3OH on a number of metal surfaces.[15–17,19,21–25,27,29,32–35] Table I shows the assignment of the vibrational bands observed in Fig. 1 for the adsorption of CH_3OH on the HOPG surface. Included for comparison are band assignments for multilayer CH_3OH adsorbed on Pd{110}[15] and Rh{100},[28] CH_3OH contained in an Ar matrix[37] and crystalline CH_3OH.[39]

The CH_3OH multilayer formed on HOPG exhibits very strong intermolecular hydrogen bonding, as demonstrated by the broadness of the O–H stretch at 3260 cm^{-1}. In addition, the O–H stretch is down shifted by ~ 400 cm^{-1} from the gas

TABLE I. Table showing the assignment of the vibrational bands observed for CH_3OH adsorbed on the HOPG surface at 97 K (Fig. 1). Also included is an assignment of the bands observed when an overlayer of CH_3OH, adsorbed at 97 K, is annealed to 130 K (Fig. 3) and the bands observed when CH_3OH is directly adsorbed at 130 K. Included for comparison are band assignments made for multilayer CH_3OH adsorbed on Pd{110} (Ref. 15) and Rh{100} (Ref. 28), CH_3OH contained in an Ar matrix (Ref. 37), and the α phase of crystalline CH_3OH (Ref. 39).

| Band assignment	Multilayer CH_3OH/HOPG at 97 K	Annealed multilayer CH_3OH/HOPG or CH_3OH adsorbed at 130 K	Multilayer CH_3OH/Pd{110}[a]	Multilayer CH_3OH/Rh{100}[b]	CH_3OH in an Ar matrix[c]	α phase of crystalline CH_3OH[d]
ν(O–H)	3260	3290	3301	3245	3667	3284
		3174	3193			3187
$\nu_a(CH_3)$	2983	2983	2987	2980	3006	2982
	2956	2958	2959		2962	2955
						2912
$2\delta_a(CH_3)a'$	2956	2958	2959		2956	
$2\delta_a(CH_3)a''$	2908	2904			2921	
$\nu_s(CH_3)$	2833	2833	2832	2905	2848	2829
2ν(C–O)		2037	2035		2054	2040
$\delta_s(CH_3)$	1468	1475	1473	1475	1466	1458
					1452	1426
δ(COH)		1521	1516		1334	1514
		1475				1470
$\rho(CH_3)$	1132	1145	1144	1180	1145	1256
					1077	1162
						1142
ν(C–O)	1045	1037	1028	1040	1034	1046
		1027			1028	1029

[a]Reference 15.
[b]Reference 28.
[c]Reference 37.
[d]Reference 39.
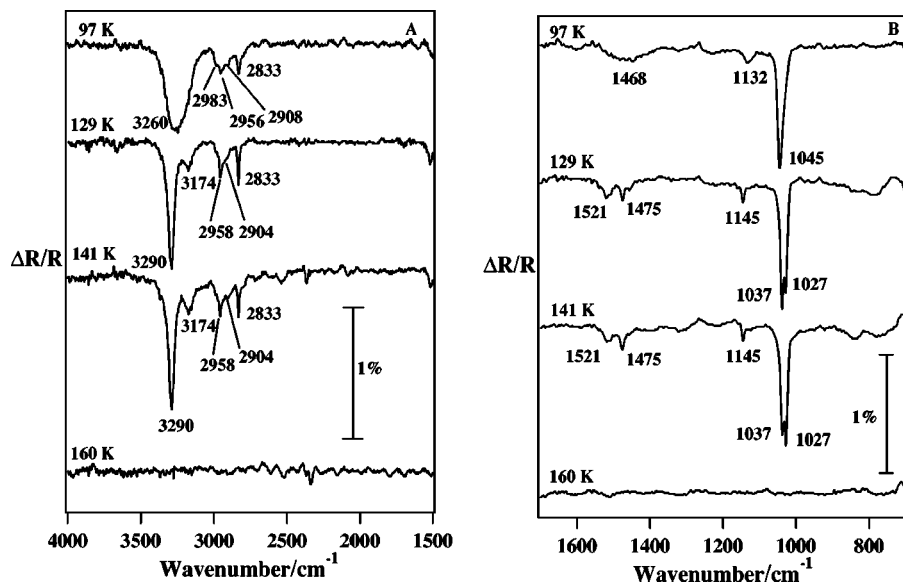
FIG. 3. RAIR spectra resulting from annealing a CH_3OH adlayer adsorbed on HOPG at 97 K. The temperatures to which the adlayer was annealed are shown on the figure. *A* shows the high frequency region of the spectrum, and *B* shows the lower frequency region of the spectrum.

phase frequency as previously observed for condensed CH_3OH phases which show hydrogen bonding.[15,39]

Figure 3 shows a series of spectra that result from annealing an overlayer produced by adsorbing 50 L of CH_3OH on HOPG at 97 K. It can clearly be seen that annealing the CH_3OH overlayer to 129 K immediately leads to the splitting of several of the bands observed in the spectrum. The O–H stretch, seen at 3260 cm^{-1}, splits into two bands at 3290 and 3174 cm^{-1}. Although these bands are sharper than the original band, they are still quite broad and appear to be superimposed on a broad background, perhaps suggesting that the feature originally observed at 3260 cm^{-1} still remains in the spectrum. The C–O stretch, originally observed at 1045 cm^{-1}, also splits on heating to give two bands at 1037 and 1027 cm^{-1}. The broad band originally observed at 1468 cm^{-1}, assigned to the asymmetric CH_3 stretch, splits on heating to give bands at 1521 and 1475 cm^{-1}. In addition to the splitting of these bands, other bands in the spectrum sharpen on annealing and the band originally observed at 1132 cm^{-1} sharpens and shifts to 1145 cm^{-1}. All of the infrared bands have disappeared from the spectra shown in Fig. 3 by 160 K, implying that the CH_3OH has desorbed from the surface by this temperature. This desorption temperature is in good agreement with observations of the adsorption of multilayer CH_3OH on Ru{001} where the physisorbed multilayer desorbed by 190 K.[25]

The splitting of bands, observed when a CH_3OH overlayer adsorbed at 97 K is annealed, can be attributed to the formation of crystalline CH_3OH on the HOPG surface. The same effect has been observed for multilayers of CH_3OH adsorbed on Ru{001},[25] polycrystalline Pt,[32] Pt{111},[34] Rh{100},[28] Pd{100},[22] Pd{110},[15] and Cu{110}.[35] Crystalline CH_3OH exists in hydrogen bonded chains in two distinct phases: the α and β phases.[40–43] Experiments have indicated that the α phase is stable below 156 K and the β phase is stable between 156 K and the melting point of CH_3OH at 175 K.[44] The two forms of crystalline CH_3OH differ in the distribution of the methyl group above and below the O atoms in the crystalline chains. For the α chains, the methyl

groups alternate above and below the O atoms allowing neighboring chains to pack closely together. In the β form, the methyl groups are randomly distributed.[45] For the α and β phases, coupling can take place between vibrations within individual chains (intrachain coupling) and for the α phase coupling can also occur between adjacent chains (interchain coupling).[15] This leads to the observed splitting in the C–O and O–H stretches.[39,45]

The assignments of the bands observed in Fig. 3, following annealing of a CH_3OH multilayer formed at 97 K, are given in Table I. The frequencies of the observed vibrations show excellent agreement with those previously measured for the α phase of crystalline CH_3OH.[39] However, it is not possible to conclusively determine whether the crystalline CH_3OH formed on HOPG adopts the α or β phase, as the vibrational structure of the two phases has not yet been fully resolved.[40,42] It is also not clear from the spectra shown in Fig. 3 whether the whole multilayer is converted to crystalline CH_3OH. In fact the bands at 3290 and 3174 cm^{-1}, which are attributed to the O–H stretch, appear to be superimposed on a broader, less intense, band suggesting that incomplete conversion of the disordered multilayer to the crystalline phase takes place. Further information concerning the conversion of disordered CH_3OH to crystalline CH_3OH was obtained from the TPD data and will be discussed later.

In addition to the observed temperature dependence, experiments also showed that the formation of crystalline CH_3OH is coverage dependant. If a multilayer that results from an exposure of 20 L of CH_3OH is annealed, no splitting of bands is observed and the overlayer that is formed simply desorbs from the surface between 150 and 160 K. However, when an overlayer resulting from a CH_3OH dose of $\geqslant$50 L is annealed, splitting is observed in the infrared spectrum and crystalline CH_3OH is formed. This is in good agreement with previous observations which showed that a minimum exposure was required before the formation of crystalline CH_3OH could be observed.[22,25,28,32,34,35]

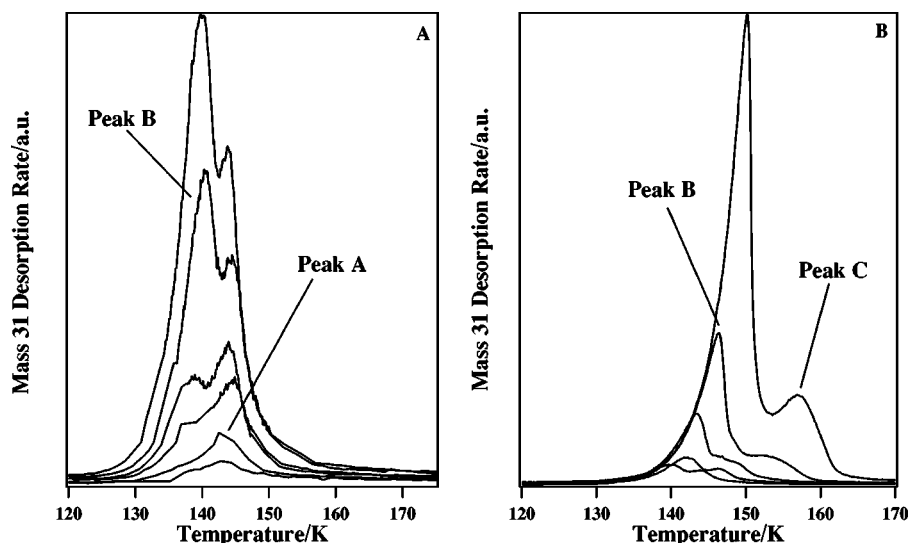Since the observation of the formation of crystalline CH_3OH was also temperature dependent, additional adsorp-

FIG. 4. TPD spectra recorded following various exposures of CH_3OH to the HOPG surface at 105 K. *A* shows TPD spectra following low CH_3OH exposures of 2, 3, 5, 7, 10, and 15 L. *B* shows spectra recorded following higher CH_3OH exposures of 15, 20, 50, 100, and 300 L.

tion experiments were performed with the surface held at 130 K. RAIR spectra were recorded as a function of increasing CH_3OH exposure. Initial adsorption of CH_3OH at lower exposures (<50 L) led to essentially identical spectra to those recorded following adsorption at 97 K (Fig. 1). The intensities of all of the vibrational bands were slightly lower for adsorption at 130 K, compared to 97 K, due to a lower sticking probability at the higher temperature. However, increasing exposures of CH_3OH (≥ 100 L) at 130 K show distinct differences compared to spectra recorded following adsorption at 97 K. Higher exposures produce spectra which are basically identical to those recorded following annealing of the adlayer formed at 97 K, with band splitting occurring in the C–O and O–H stretching modes. Splitting could only be observed for doses of $CH_3OH \geq 100$ L. Annealing the adlayer formed following CH_3OH exposure to HOPG at 130 K did not lead to the formation of any new spectral features and all vibrational bands disappeared from the spectrum by 160 K, similar to adsorption at 97 K.

B. TPD experiments

1. Results

TPD spectra were recorded following CH_3OH adsorption on HOPG at 105 and 130 K. All spectra were recorded with a linear heating rate of $0.5\ \mathrm{K\,s^{-1}}$. Spectra are shown with desorption peaks for mass 31 only. Mass 31 is the major fragment ion created in the mass spectrometer when detecting CH_3OH, and is not the result of any surface chemistry. To confirm this, the ratio of mass 32 desorption to mass 31 desorption was checked regularly and compared with the cracking pattern of CH_3OH recorded with the same mass spectrometer when CH_3OH was dosed into the UHV chamber. In all cases the ratio of mass 32 desorption to mass 31 desorption was 0.73.

A series of TPD spectra, recorded following the adsorption of CH_3OH on HOPG at 105 K, are shown in Fig. 4. Following the lowest exposures of CH_3OH (2 and 3 L) only one peak is observed with a desorption temperature of ~ 144 K. This is labeled as peak *A*. As the exposure is increased to 5 L a second, lower temperature, peak is observed,

initially as a shoulder on peak *A*. Following an exposure of 7 L, this shoulder can be clearly identified as a separate peak at ~ 139 K. This peak is labeled as peak *B*. As the exposure is further increased to 10 and 15 L, peak *B* begins to dominate the spectrum. The desorption temperature of peak *B* also increases with increasing CH_3OH exposure. Figure 4(b) shows TPD spectra following higher exposures of CH_3OH to the surface. It is clear that, with increasing exposure, peaks *A* and *B* merge into one and the resulting peak continues to grow and shift up in temperature. As the exposure is increased above 50 L, an additional peak (peak *C*) is observed at around 157 K. Increasing exposure causes peak *C* to grow in intensity and shift up in temperature. Peaks *B* and *C* cannot be saturated.

Peak *A* is assigned to the desorption of CH_3OH from a physisorbed monolayer adsorbed on the HOPG surface. This peak is the first to appear in the spectrum and hence must be due to CH_3OH that is closely associated with the surface. Peaks *B* and *C* are assigned to the desorption of multilayer CH_3OH from the HOPG surface. It is noted that the desorption of multilayers should be a zero-order process and that the resulting TPD spectra should therefore share a leading edge. However, it is clear from Figs. 4(a) and 4(b) that the spectra do not share a leading edge, suggesting a fractional order desorption process as previously observed for CH_3OH adsorbed on Pd{100},[22] NiO,[36] and Al_2O_3.[46] This point will be discussed in more detail later.

As RAIR spectra recorded following CH_3OH adsorption at 130 K showed distinct differences compared to those recorded for 97 K adsorption, TPD spectra were also recorded following higher temperature adsorption. Figure 5 shows TPD spectra recorded following CH_3OH adsorption on HOPG at 130 K. The spectra seen in Fig. 5 are very similar to those in Fig. 4, with a few small differences. Hence, the species giving rise to the three desorption peaks observed in Fig. 5 are assigned to the same species as observed following adsorption at 105 K. The first difference between the spectra in Fig. 5 and those in Fig. 4 is that peak *B* is observed to grow into the spectrum at slightly higher exposures when CH_3OH is adsorbed at 130 K. This is due to a lower sticking
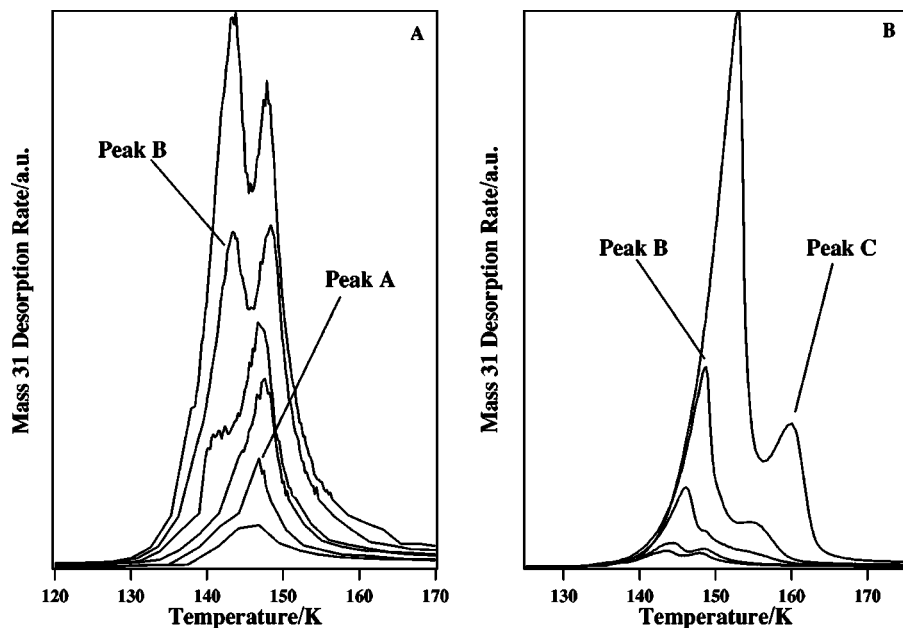
FIG. 5. TPD spectra recorded following various exposures of CH_3OH to the HOPG surface at 130 K. *A* shows TPD spectra following low CH_3OH exposures of 2, 3, 5, 7, 10, and 15 L. *B* shows spectra recorded following higher CH_3OH exposures of 15, 20, 50, 100, and 300 L.

probability at the higher adsorption temperature. The desorption temperatures for the peaks seen in Fig. 5 are also a few degrees higher than those observed following adsorption at 105 K. This could be due to differing amounts of hydrogen bonding in the overlayers formed at 105 and 130 K. This is supported by the RAIR spectra recorded following adsorption at 130 K, which show a slightly higher vibrational frequency for the O–H stretch, which is very sensitive to the amount of hydrogen bonding present in the system. The final difference between the spectra in Fig. 5 and those in Fig. 4, is the more pronounced nature of peak *C* following adsorption at 130 K [Fig. 5(b)] compared to adsorption at 105 K [Fig. 4(b)]. This will be discussed in more detail later.

2. Peak fitting

In order to obtain quantitative information about the desorption of CH_3OH from the HOPG surface, it is necessary to separate the TPD spectra into individual peaks so that the contributions from different desorbing species can be evaluated. This requires that the recorded TPD spectra are peak fitted. The package used to fit the experimental data was IGOR Pro (version 5.00, Wavemetrics Inc.). A Lorentzian peak shape was chosen to fit the data as this gave the smallest chi squared value for individual fits, and hence the most accurate overall fit. Since the baselines of the TPD spectra were not perfectly flat, the baseline was also fitted with a cubic polynomial function. For all of the data, the number of peaks used in the fit reflected the actual number of peaks observed in the TPD spectrum. Hence, for the 2 and 3 L spectra only one peak is used for the fit (peak *A*), while two peaks are used to fit the spectra recorded following CH_3OH exposures of 5–20 L (peaks *A* and *B*). For exposures of 50 L and above it was not possible to distinguish peaks *A* and *B* and therefore two peaks were used to fit these spectra: peaks *A/B* and peak *C*. The error introduced by neglecting peak *A* at higher exposures is small as, at these exposures, peak *A* comprises only around 3% of the total peak area. For both

105 and 130 K adsorption, two sets of data were fitted and analyzed to both check the reproducibility of the results and to check the quality of the fitting procedure. Figure 6 shows an example of a fit to the TPD data recorded following a 15 L exposure of CH_3OH to the HOPG surface at 105 K. It is clear from Fig. 6 that the quality of the fit is very good. It was possible to achieve fits of the same quality for all spectra recorded following dosing at both 105 and 130 K.

To further determine the accuracy of the peak fitting procedure, certain key features such as the peak area and peak temperature of the measured and fitted TPD curves were calculated and compared. Peak temperatures were found to be in good agreement between the measured and fitted data. Figure 7 shows a comparison of the integrated area as a function of exposure for measured and fitted TPD data resulting from CH_3OH adsorption at 105 K on the HOPG surface. It is clear that the agreement between the two sets of integrated areas is good.
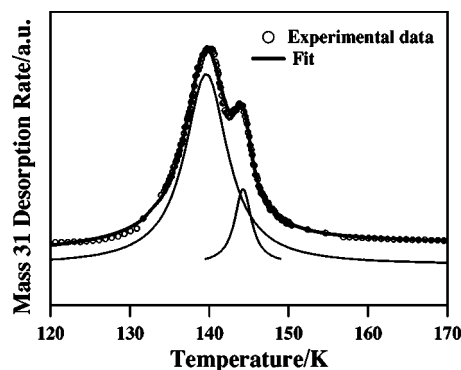

FIG. 6. Figure showing an example of a peak fit to experimental data recorded following a CH_3OH exposure of 15 L to the HOPG surface at 105 K. The TPD spectrum has been fitted with two baseline corrected Lorentzian functions. The dots represent the experimental data, the thin lines represent the individual Lorentzian functions, and the thick line shows the total combined fit to the experimental data.
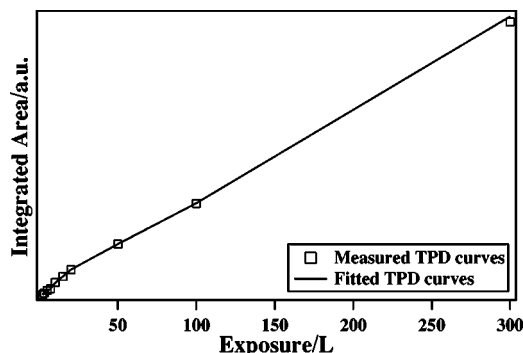
FIG. 7. Graph showing the integrated area, as a function of CH_3OH exposure, of the experimentally measured and fitted TPD curves obtained following CH_3OH adsorption on HOPG at 105 K. Good agreement is obtained between the areas calculated for both sets of data. This graph also shows that the sticking probability of CH_3OH on the HOPG surface is approximately constant over the whole exposure range.

3. Uptake curves

Figure 7 shows the total uptake of CH_3OH on the HOPG surface at 105 K as a function of increasing CH_3OH exposure. It is clear that the uptake of CH_3OH is fairly linear, implying a constant sticking probability as a function of exposure. This is characteristic of physisorption. As well as determining the total uptake of CH_3OH, it was also possible to determine the relative coverage of each desorbing species as a function of exposure, once a good fit to the measured TPD data had been achieved. The relative coverage for each species was evaluated by integrating the area under the individual TPD peaks produced from the peak fitting procedure. It was only possible to determine relative coverage and not absolute coverage as our current experimental setup does not allow a measurement of the actual coverage on the surface.

Figure 8 shows the integrated areas of peaks A, B, and C as a function of exposure following adsorption at 105 K. The data shown are the average of two sets of data. Similar curves, showing virtually identical trends, can also be produced for data recorded following adsorption at 130 K. It is
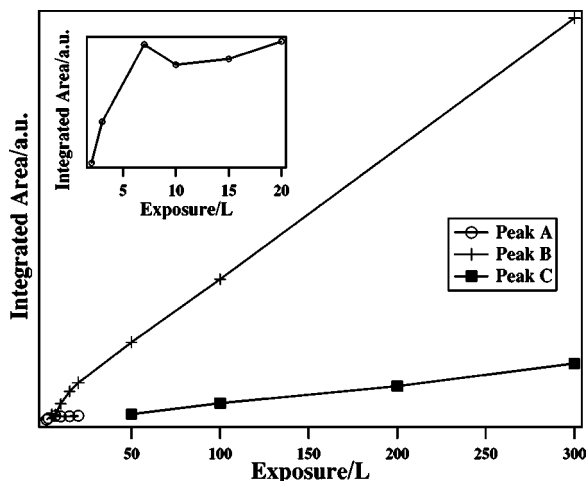
clear from Fig. 8 that the relative coverage of the species giving rise to peaks B and C increases fairly linearly with exposure and does not saturate. This confirms the assignment of these peaks to the desorption of multilayer CH_3OH from the surface. The exact nature of the multilayer species giving rise to peaks B and C is discussed in more detail later. The inset in Fig. 8 shows a close up of the integrated area of peak A as a function of increasing CH_3OH exposure. It is clear that the area of peak A increases as the exposure is increased from 2 to 7 L, indicating that the relative coverage of this species on the surface also increases. However, for exposures of 10 L and above, the integrated area of peak A saturates. This confirms the assignment of this peak to the desorption of a monolayer of CH_3OH from the HOPG surface. The fact that the desorption of monolayer CH_3OH can be distinguished from multilayer CH_3OH indicates that, although weak, the bonding between CH_3OH and the surface is slightly stronger than the bonding between two CH_3OH molecules that occurs in the multilayer. The same effects are also seen following adsorption at 130 K. However, peak A is observed to saturate at a slightly higher exposure due to the lower sticking probability at the higher adsorption temperature. The monolayer saturation coverage is, however, similar for adsorption at 105 and 130 K as the integrated area under peak A saturates at approximately the same value in both cases.

Figure 8 also shows that multilayers of CH_3OH on the HOPG surface begin to grow even before the monolayer is saturated, as peak B becomes populated before peak A saturates. This effect has previously been observed for CH_3OH adsorbed on HOPG[8] and also on NiO[36] and Al_2O_3.[46] This observation further suggests that the desorption of CH_3OH multilayers from the HOPG surface is not a perfect zero-order process. Multilayers which desorb with zero-order kinetics are seen to adsorb and desorb in a layer-by-layer fashion which is clearly not the case here. Since the bonding of CH_3OH to the HOPG surface is observed to be slightly stronger than that of CH_3OH to another CH_3OH molecule, it is assumed that this "islanding" of molecules occurs due to a lack of mobility at this adsorption temperature, rather than due to an energetic effect.

4. Desorption orders

In order to gain a deeper understanding of the desorption kinetics for CH_3OH adsorbed on HOPG, the desorption order for each of the individual desorbing species has been determined. Thermal desorption is described by the Polanyi–Wigner equation:[47–49]

$$r_{des} = -\frac{d\theta}{dt} = \nu_n \theta^n \exp\left(\frac{-E_{des}}{RT}\right), \qquad (1)$$

where r_{des} is the rate of desorption, ν_n is the preexponential factor for the desorption process of order n, θ is the coverage, E_{des} is the desorption activation energy, R is the gas constant, and T is the surface temperature. The rate of change of coverage θ with time t can be linked to the rate of change of coverage with temperature via the TPD heating rate β,

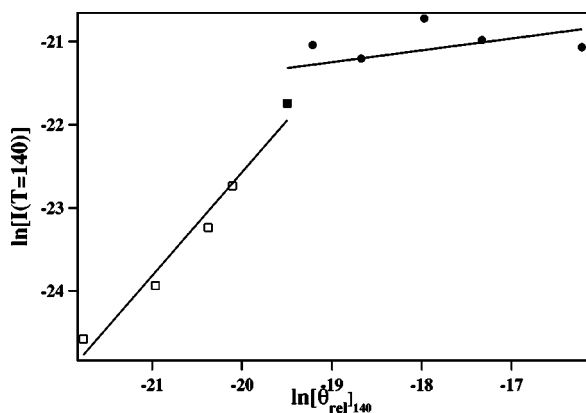

FIG. 8. Graph showing the integrated areas of the individual peaks that make up the TPD spectra recorded following CH_3OH adsorption on HOPG at 105 K. The inset shows a close up of the data for peak A, the monolayer peak.

FIG. 9. A plot of $\ln[I(T=140)]$ against $\ln[\theta_{rel}]_{140}$ for the data shown in Fig. 4. This graph allows the order of desorption to be determined from the gradient of the plot. The open squares represent the data for exposures between 2 and 10 L (the monolayer) and the filled circles are for exposures of 15 L and above (the multilayer).

$$\frac{d\theta}{dt} = \frac{d\theta}{dT} \times \frac{dT}{dt} = \frac{d\theta}{dT}\beta. \tag{2}$$

In TPD experiments, the rate of change of coverage with temperature is proportional to the intensity of the measured TPD trace I(T). In the experiments described here it is not possible to measure an absolute coverage, however integrating the area under the TPD peaks does allow a relative coverage θ_{rel}, to be obtained. Hence Eq. (1) can now be rewritten as

$$I(T) \propto \nu_n \theta_{rel}^n \exp\left(\frac{-E_{des}}{RT}\right). \tag{3}$$

Taking logarithms of both sides of this equation leads to Eq. (4)

$$\ln[I(T)] \propto n\ln[\nu_n\theta_{rel}] - \frac{E_{des}}{RT}. \tag{4}$$

At a fixed temperature, here defined as T_x, Eq. (4) shows that the order of desorption can be determined by performing a plot of $\ln[I(T_x)]$ against $\ln[\theta_{rel}]_{Tx}$. The gradient of this graph will give n, the order of desorption.[48] Note that in order to perform this plot it is necessary to assume that the preexponential factor and the desorption energy do not vary with coverage or with temperature. This is a good assumption for the preexponential factor, as all of the CH_3OH is physisorbed on the surface. This is also an acceptable assumption for the desorption energy which shows only a weak variation with coverage (see later).

Figure 9 shows a plot of $\ln[I(T_x)]$ against $\ln[\theta_{rel}]_{Tx}$ for a T_x value of 140 K for CH_3OH adsorption on HOPG at 105 K. This value of T_x was chosen to ensure that sufficient intensity in both the monolayer peak (peak A) and the multilayer peak (peak B) could be obtained with increasing exposure. Note that this plot was produced directly from the experimental data and not from the fitted TPD data. It is obvious from Fig. 9 that there is a different gradient in this plot for exposures ≤ 10 L (open squares) and for exposures above 10 L (filled circles). The reason for this can clearly be seen by looking at Fig. 4 which shows that for the lower

TABLE II. Table showing the calculated order of desorption for the monolayer and multilayer peaks (peaks A and B) observed in the TPD spectra that result from the exposure of the HOPG surface to CH_3OH. The numbers given in the table are the average values obtained from analyzing four separate sets of data. The order of desorption n is obtained from the gradient of a plot of $\ln[I(T_x)]$ against $\ln[\theta_{rel}]_{Tx}$ at a fixed temperature T_x. An example of such a plot is shown in Fig. 9.

T_x (K)	n for peak A (monolayer)	n for peak B (multilayer)
140	1.28	0.17
142.5	1.09	0.46
145	1.31	0.41

exposures (<10 L) the chosen T_x value passes through peak A (the monolayer peak), while for exposures above 10 L the chosen T_x value passes through peak B (the multilayer peak). Figure 9 therefore shows that, as expected, the order of desorption is different for monolayer and multilayer CH_3OH. The gradients of the graph shown in Fig. 9 give a desorption order of 1.24 for peak A (the monolayer peak) and 0.14 for peak B (the multilayer peak). In order to check the accuracy of these values, this process was repeated for a variety of fixed temperatures T_x and for a range of TPD data sets. The gradients of the resulting graphs, and hence the desorption orders for the monolayer and multilayer peaks, are given in Table II. The data in Table II are the average desorption orders that result from the analysis of four sets of TPD data recorded following adsorption at both 105 and 130 K.

Analysis of all T_x values shows that peak A has a desorption order of 1.23 ± 0.14, again confirming its assignment to the desorption of monolayer CH_3OH. Since CH_3OH has been shown to adsorb reversibly on HOPG, first-order desorption would be expected and a desorption order of one has previously been used to model CH_3OH desorption from a monolayer adsorbed on Al_2O_3.[46] A first-order desorption process assumes that each desorbing molecule is not influenced by surrounding molecules on the surface. The value of 1.23 ± 0.14, determined here for monolayer CH_3OH desorption from HOPG, is slightly higher than the expected value of 1. This can be attributed to interactions, such as hydrogen bonding, that occur within the monolayer. Peak B has a calculated desorption order of 0.35 ± 0.21, in excellent agreement with other studies which have shown that multilayer CH_3OH desorption is a fractional order process.[22,36,46] The observation of a fractional desorption order for multilayer CH_3OH desorption from HOPG is supported by the fact that TPD spectra for increasing doses of CH_3OH (seen in Figs. 4 and 5) do not share leading edges as would be expected for perfect zero-order desorption. The observed fractional order desorption for peak B (the multilayer peak) is assigned to the presence of hydrogen bonding in the CH_3OH multilayer that leads to strong interactions between adjacent molecules. The infrared spectra (shown in Fig. 1) also show evidence of strong hydrogen bonding as shown by the vibrational frequency and broadness of the O–H stretching band. Note that desorption orders have not been calculated for the second multilayer species that gives rise to peak C. This is because this peak only appears in the spectra at relatively high
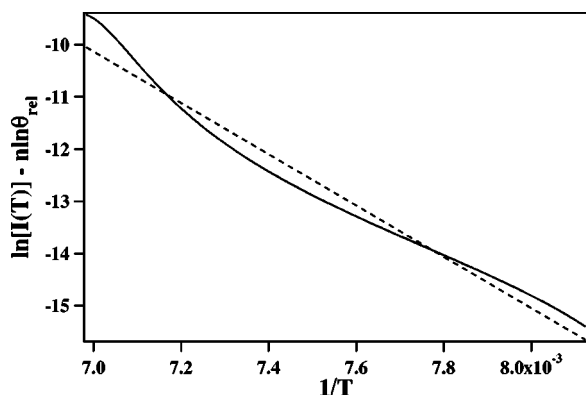
FIG. 10. A graph of $(\ln[I(T)] - n \ln \theta_{rel})$ against $1/T$ for a multilayer of CH_3OH adsorbed on HOPG following a 50 L exposure at 105 K. This graph was plotted with a desorption order of 0.35. The gradient of the graph is equal to $-E_{des}/R$ and allows a value for the desorption energy to be obtained. The solid line shows the actual data points and the dashed line shows a fit to this data that allows the gradient to be determined.

CH_3OH doses and therefore there is only a small amount of data for this peak. In addition, it is thought that this TPD peak partially arises due to the heating process in the TPD experiment (see later).

5. Desorption energies

As well as obtaining the order of desorption, it is also possible to determine the desorption energy for CH_3OH adsorbed on HOPG. This gives an indication of the strength of the binding of CH_3OH, both to the HOPG surface and within the multilayer.

Equation (4) can be rewritten as follows:

$$\ln[I(T)] \propto n \ln v_n + n \ln \theta_{rel} - \frac{E_{des}}{RT}. \quad (5)$$

Further rearrangement then gives Eq. (6):

$$\ln[I(T)] - n \ln \theta_{rel} \propto n \ln v_n - \frac{E_{des}}{RT}. \quad (6)$$

Hence plotting $(\ln[I(T)] - n \ln \theta_{rel})$ against $1/T$ should give a straight line with a gradient of $-E_{des}/R$. Again this assumes that the preexponential factor is constant, a good assumption given that CH_3OH is physisorbed on HOPG at all coverages. Note that the intercept cannot be used to give a value for the preexponential factor v_n as the coverage is only a relative coverage. In order to obtain a value for v_n from a plot of this type, it is necessary to know the absolute coverage.

Figure 10 shows a plot of $(\ln[I(T)] - n \ln \theta_{rel})$ against $1/T$ for the multilayer, following a 50 L exposure of CH_3OH to HOPG at 105 K. Note that in order to plot this graph, it was necessary to separate out the contributions of the different TPD peaks (A, B, and C) and hence this plot is performed for the peak fitted TPD data not the raw data. Similar plots were performed for both the monolayer species (peak A) and the multilayer species (peak B) using the range of n values already determined. These plots were performed for several sets of TPD data, in order to obtain average values for the desorption energies.

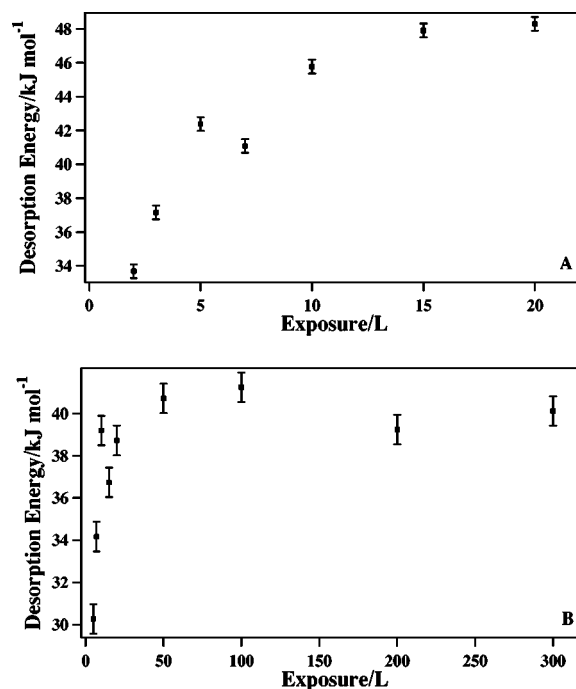Figure 11 shows how the calculated desorption energy

FIG. 11. Graphs showing the variation of the desorption energy of CH_3OH on the HOPG surface for A the monolayer and B the multilayer as a function of exposure at 105 K. The data points represent the average desorption energy calculated from several sets of TPD data. The error bars represent the error that arises from the uncertainty in the value of the desorption order n.

for both the monolayer [Fig. 11(a)] and the multilayer [Fig. 11(b)] vary as a function of CH_3OH exposure on HOPG at 105 K. The data points represent the average desorption energy calculated from several sets of TPD data, and the error bars represent the error in the calculated desorption energy that arises from the uncertainty in the value of the desorption order n. Data for 130 K adsorption are not shown here but show very similar results. As for the desorption orders, no value of the desorption energy has been calculated for peak C. Figure 11(a) shows that the desorption energy for the monolayer (peak A) increases from ≈ 33 to 48 kJ mol^{-1} as the CH_3OH exposure increases from 2 to 20 L. This desorption energy corresponds either to a strongly physisorbed species or to a weakly chemisorbed species. However, the RAIR spectra also recorded for this adsorption system suggest that chemisorbed CH_3OH is not adsorbed on the HOPG surface and hence it is assumed that the CH_3OH monolayer is, instead, strongly physisorbed. The observed increase in desorption energy with increasing exposure indicates that the CH_3OH becomes more strongly bound as the coverage increases. It is most likely that this is due to increasing amounts of hydrogen bonding between the CH_3OH molecules that becomes possible as the coverage increases.

Figure 11(b) shows the desorption energy for the multilayer peak, peak B, as a function of increasing CH_3OH exposure. It is clear that the multilayer desorption energy also increases with increasing coverage from 31 kJ mol^{-1} up to around 40 kJ mol^{-1} following a 300 L CH_3OH exposure. Again this corresponds to the desorption of a physisorbed species and is in good agreement with desorption energies of 30.2 and 37.7 kJ mol^{-1} previously reported for two phys-

isorbed states of CH_3OH desorbing from Pd{100}.[22] This desorption energy is also in good agreement with the enthalpy of sublimation of CH_3OH which is $44.9 \, kJ \, mol^{-1}$.[46] It is noted that, as expected, at all CH_3OH exposures the calculated desorption energy is larger for the monolayer than for the multilayer. As for the monolayer, it is assumed that the observed increase in the desorption energy with increasing coverage can be assigned to the larger amounts of hydrogen bonding that occur within the multilayer at higher CH_3OH exposures.

The data in Fig. 11(b) suggest two possible regimes for the adsorption of multilayer CH_3OH. Initially, the desorption energy of the multilayer increases rapidly with increasing CH_3OH exposure, but at an exposure above 10–20 L the desorption energy seems to plateau. Previous investigations have suggested the formation of an intermediate or "sandwich" phase of CH_3OH[15] in which the lattice mismatch between bulk CH_3OH ice and the CH_3OH that is bound to the surface is accommodated. It is therefore suggested that it is this intermediate phase of disordered multilayer CH_3OH that shows the rapid increase in desorption energy, due to the formation of increasing amounts of hydrogen bonding as the multilayer grows. The approximately constant desorption energy, observed above CH_3OH doses of 10–20 L, occurs due to the subsequent formation of more ordered CH_3OH overlayers in which the amount of hydrogen bonding remains constant with increasing exposure.

6. Model for the adsorption of CH₃OH on HOPG

Putting together the data obtained from both RAIRS and TPD allows a model of the adsorption of CH_3OH on HOPG to be developed. RAIR spectra have shown that CH_3OH is always physisorbed on the HOPG surface and that crystalline CH_3OH can be formed provided the surface temperature and coverage are high enough. TPD data shows that it is possible to distinguish the desorption of monolayer CH_3OH (peak A, Fig. 4) and multilayer CH_3OH (peaks B and C, Fig. 4). Peaks B and C have both been assigned to the desorption of multilayer CH_3OH, however, the difference between these two multilayer species needs to be determined.

A possible assignment for peak C uses information obtained from the RAIR spectra. As already discussed, the formation of crystalline CH_3OH can be observed with RAIRS either upon annealing the surface after adsorption at 97 K, or following adsorption to high exposures at 130 K. The TPD spectra seen in Figs. 4(b) and 5(b) show that peak C is only observed at CH_3OH exposures $\geqslant 50 \, L$ in both the 100 and 130 K TPD spectra. This peak is therefore assigned to the desorption of crystalline multilayer CH_3OH. Note that no crystalline CH_3OH is formed on the surface during adsorption at 105 K, irrespective of exposure. However, during the TPD process some of the CH_3OH multilayer is converted to crystalline CH_3OH which then desorbs as a separate peak. In agreement with the RAIRS data, where crystalline CH_3OH could not be formed for exposures $< 50 \, L$, peak C only appears in the TPD spectrum for CH_3OH exposures of 50 L and above.

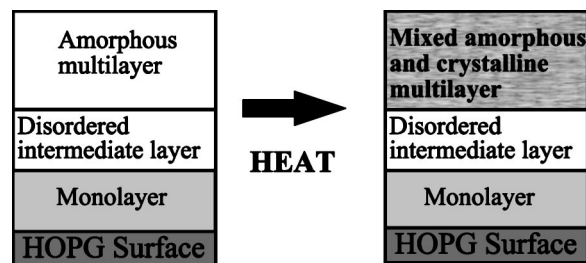The assignment of peak C to the formation, and subsequent desorption, of crystalline CH_3OH is supported by the

FIG. 12. A schematic diagram showing how CH_3OH is adsorbed on HOPG at 100 K and what happens to the resulting overlayer when heating occurs. The overlayer produced following annealing of an adlayer adsorbed at 100 K is very similar to that produced when CH_3OH is adsorbed at 130 K.

observation that following CH_3OH adsorption at 130 K, the TPD spectra show a more pronounced peak C [Fig. 5(b)]. This arises due to the fact that some crystalline CH_3OH is actually formed during adsorption as well as being formed during the TPD experiment, leading to the desorption of larger amounts of crystalline CH_3OH. Hence, in the TPD spectra shown in Figs. 4 and 5, peak B is assigned to the desorption of disordered, or amorphous, multilayer CH_3OH and peak C is assigned to the desorption of crystalline CH_3OH. It would be expected that crystalline CH_3OH desorbs at a higher temperature than amorphous CH_3OH due to the larger number of hydrogen bonds present in the highly ordered crystalline structure. Note that initial inspection of the RAIR spectra seen in Fig. 3 suggests that all of the disordered CH_3OH converts to crystalline CH_3OH on annealing, a fact that is clearly in disagreement with the TPD data. However, closer inspection of the RAIR spectra in Fig. 3 shows that the sharper peaks observed in the O–H region of the spectrum are superimposed on a broad band which is assigned to the presence of disordered CH_3OH multilayers. Therefore it is suggested that disordered and crystalline multilayers coexist on the surface. In addition, annealing in the RAIRS experiments was done in a rather different manner to the heating in the TPD experiments and therefore it is very likely that more CH_3OH could be converted to the crystalline form in the RAIRS experiment compared to in the TPD experiments.

It is now possible to build up a picture of the adsorption of CH_3OH on the HOPG surface and Fig. 12 shows a schematic diagram of this model. When CH_3OH is adsorbed on HOPG at $\sim 100 \, K$, initial adsorption leads to the formation of a physisorbed monolayer. Subsequent adsorption leads to the formation of first an intermediate multilayer, and subsequently a disordered, or amorphous, multilayer. These two multilayers cannot be distinguished from one another in the TPD spectrum and both give rise to peak B. Annealing this adlayer (either in a RAIRS experiment or during the TPD experiment) leads to the formation of a mixed crystalline and amorphous overlayer. The crystalline CH_3OH desorbs at a higher temperature than the amorphous CH_3OH due to it having a more ordered structure. Adsorption at 130 K essentially leads to the formation of a CH_3OH adlayer that is very similar to that formed when an adlayer adsorbed at $\sim 100 \, K$ is annealed, hence accounting for the marked similarity between the TPD data shown in Figs. 4 and 5. Note that the

TPD data show that only around 20%–30% of the CH_3OH multilayer is converted to crystalline CH_3OH as peak C has an integrated area that is much smaller than that of peak B.

Previous work[15] for CH_3OH adsorbed on Pd{110} has suggested that it is not possible to distinguish between the desorption of amorphous and crystalline CH_3OH. This is clearly not the case here, however this difference could be due to the different heating rates used in this experiment and the previous experiment.[15] An alternative model was also suggested for the growth of CH_3OH adlayers on Ag{111}.[33] This model suggested that crystalline CH_3OH desorbs at a lower temperature than amorphous CH_3OH.[33] However, this cannot be the case for CH_3OH desorbing from HOPG as, in this case, peak B would be due to the desorption of crystalline CH_3OH and peak C would be due to the desorption of amorphous CH_3OH. However, peak B is observed to appear in the TPD spectra shown in Figs. 4 and 5 following a CH_3OH exposure of only 7–10 L. This is clearly much lower than the exposure at which the formation of crystalline CH_3OH is observed with RAIRS and therefore indicates that this alternative model cannot hold for CH_3OH adsorbed on the HOPG surface.

IV. SUMMARY AND CONCLUSIONS

RAIRS and TPD data have shown that CH_3OH is physisorbed on HOPG at all coverages and that crystalline CH_3OH can also be formed provided the coverage is high enough. Three desorbing species have been observed with TPD, as a function of increasing exposure, which are assigned to the desorption of a monolayer, an amorphous multilayer, and a crystalline multilayer. The monolayer has a desorption order of 1.23 ± 0.14 and a desorption energy that rises from 33 to 48 kJ mol^{-1} with increasing CH_3OH exposure. The disordered multilayer has a much smaller desorption order of 0.35 ± 0.21 and a desorption energy that also rises as a function of exposure from 31 kJ mol^{-1} at low CH_3OH exposures to ~ 40 kJ mol^{-1} at high coverages.

Hydrogen bonding between the CH_3OH molecules is found to have a strong influence on the behavior of CH_3OH adsorbed on HOPG. It is thought that it is the presence of hydrogen bonding between adjacent molecules that causes the observed increase in the desorption energy as a function of increasing coverage in both the monolayer and the multilayer. It is also the presence of hydrogen bonding within the overlayer that leads to the observation of a non-zero desorption order for the multilayer. In addition, the multilayer is seen to grow on the HOPG surface even before the monolayer has saturated, again indicating that the formation of hydrogen bonds between the CH_3OH molecules plays an important role in its adsorption on the HOPG surface. However, at low doses of CH_3OH on the HOPG surface it is possible to distinguish between the desorption of a monolayer and a multilayer, implying that hydrogen bonding is not always dominant for CH_3OH adsorption on HOPG. In fact, the binding of the CH_3OH to the HOPG surface must be slightly stronger than the binding between CH_3OH molecules in the bulk ice, otherwise it would not be possible to distinguish between monolayer and multilayer adsorption.

The results described here form part of a wider study of the adsorption and formation of a range of astrochemically relevant molecules on dust grain analog surfaces. Whilst the experiments described here were performed at 100 K, as opposed to 10–20 K which is the temperature of dust grains in the ISM, they still provide detailed information about the formation of CH_3OH ices on grain surfaces and about the subsequent desorption of these ices from the grains. This information is crucially important for astronomical models of the star formation process and the data from this study will be incorporated into suitable astronomical models.[50] Similar TPD results have previously been successfully incorporated into astronomical models[51] of the star formation process.

[1] D. A. Williams, in *Dust and Chemistry in Astronomy*, edited by T. J. Millar and D. A. Williams (Institute of Physics, Bristol, 1993).

[2] A. G. G. M. Tielens and D. C. B. Whittet, in *Molecules in Astrophysics: Probe and Process*, edited by E. F. van Dishoeck (Kluwer, Dordrecht, 1997).

[3] S. B. Charnley, A. G. G. M. Tielens, and S. D. Rodgers, ApJ **482**, L203 (1997).

[4] J. S. A. Perry and S. D. Price, Astrophys. Space Sci. **285**, 769 (2003).

[5] V. Pirronello, C. Liu, J. E. Roser, and G. Vidali, Astron. Astrophys. **344**, 681 (1999).

[6] J. S. A. Perry, J. M. Gingell, K. A. Newson, J. To, N. Watanabe, and S. D. Price, Meas. Sci. Technol. **13**, 1414 (2002).

[7] N. Katz, I. Furman, O. Biham, V. Pirronello, and G. Vidali, Astrophys. J. **522**, 305 (1999).

[8] L. Wang, Y. H. Song, A. G. Wu, Z. Li, B. L. Zhang, and E. K. Wang, Appl. Surf. Sci. **199**, 67 (2002).

[9] A. Y. Rozovskii and G. I. Lin, Top. Catal. **22**, 137 (2003).

[10] R. I. Masel, *Principles of Adsorption and Reactions on Solid Surfaces* (Wiley, New York, 1996).

[11] M. Stoukides, Catal. Rev. - Sci. Eng. **42**, 1 (2000).

[12] R. B. Barros, A. R. Garcia, and L. M. Ilharco, J. Phys. Chem. B **108**, 4831 (2004).

[13] F. P. Netzer and M. G. Ramsey, Crit. Rev. Solid State Mater. Sci. **17**, 397 (1992).

[14] R. Shekhar and M. A. Barteau, Catal. Lett. **31**, 221 (1995).

[15] S. J. Pratt, D. K. Escott, and D. A. King, J. Chem. Phys. **119**, 10867 (2003).

[16] A. K. Bhattacharya, M. A. Chesters, M. E. Pemble, and N. Sheppard, Surf. Sci. **206**, L845 (1988).

[17] R. B. Barros, A. R. Garcia, and L. M. Ilharco, Surf. Sci. **502−503**, 156 (2002).

[18] R. B. Barros, A. R. Garcia, and L. M. Ilharco, Surf. Sci. **532−535**, 185 (2003).

[19] G. Krenn and R. Schennach, J. Chem. Phys. **120**, 5729 (2004).

[20] V. Efstathiou and D. P. Woodruff, Surf. Sci. **526**, 19 (2003).

[21] S. M. Johnston, A. Mulligan, V. Dhanak, and M. F. Kadodwala, Surf. Sci. **530**, 111 (2003).

[22] K. Christmann and J. E. Demuth, J. Chem. Phys. **76**, 6308 (1982).

[23] J. E. Demuth and H. Ibach, Chem. Phys. Lett. **60**, 395 (1979).

[24] S. A. Sardar, J. A. Syed, K. Tanaka, F. P. Netzer, and M. G. Ramsey, Surf. Sci. **519**, 218 (2002).

[25] J. Hrbek, R. A. De Paola, and F. M. Hoffmann, J. Chem. Phys. **81**, 2818 (1984).

[26] K. Christmann and J. E. Demuth, J. Chem. Phys. **76**, 6318 (1982).

[27] J. P. Camplin and E. M. McCash, Surf. Sci. **360**, 229 (1996).

[28] J. E. Parmeter, X. D. Jiang, and D. W. Goodman, Surf. Sci. **240**, 85 (1990).

[29] R. B. Barros, A. R. Garcia, and L. M. Ilharco, J. Phys. Chem. B **105**, 11186 (2001).

[30] W. S. Sim, P. Gardner, and D. A. King, J. Phys. Chem. **99**, 16002 (1995).

[31] I. E. Wachs and R. J. Madix, J. Catal. **53**, 208 (1978).

[32] A. Peremans, F. Maseri, J. Darville, and J. M. Gilles, Surf. Sci. **227**, 73 (1990).

[33] H. G. Jenniskens, P. W. F. Dorlandt, M. F. Kadodwala, and A. W. Kleyn, Surf. Sci. **358**, 624 (1996).

[34] D. H. Ehlers, A. Spitzer, and H. Luth, Surf. Sci. **160**, 57 (1985).

[35] A. Peremans, F. Maseri, J. Darville, and J. M. Gilles, J. Vac. Sci. Technol. A **8**, 3224 (1990).

[36] M. Wu, C. M. Truong, and D. W. Goodman, J. Phys. Chem. **97**, 9425 (1993).

[37] A. Serrallach, R. Meyer, and H. H. Gunthard, J. Mol. Spectrosc. **52**, 94 (1974).

[38] J. Heidberg and M. Warskulat, J. Electron Spectrosc. Relat. Phenom. **54/55**, 961 (1990).

[39] M. Falk and E. Whalley, J. Chem. Phys. **34**, 1554 (1961).

[40] P. Robyr, B. H. Meier, P. Fischer, and R. R. Ernst, J. Am. Chem. Soc. **116**, 5315 (1994).

[41] B. H. Torrie, O. S. Binbrek, M. Strauss, and I. P. Swainson, J. Solid State Chem. **166**, 415 (2002).

[42] B. H. Torrie, S. X. Weng, and B. M. Powell, Mol. Phys. **67**, 575 (1989).

[43] K. J. Tauer and W. N. Lipscomb, Acta Crystallogr. **5**, 606 (1952).

[44] L. A. K. Staveley and M. A. P. Hogg, J. Chem. Soc. **1013**, (1954).

[45] F. Fischer and R. Fuhrich, Z. Naturforsch. A **38**, 31 (1983).

[46] S. Y. Nishimura, R. F. Gibbons, and N. J. Tro, J. Phys. Chem. B **102**, 6831 (1998).

[47] D. A. King, Surf. Sci. **47**, 384 (1975).

[48] A. M. de Jong and J. W. Niemantsverdriet, Surf. Sci. **233**, 355 (1990).

[49] J. B. Miller, H. R. Siddiqui, S. M. Gates, J. N. J. Russell, J. T. Yates, Jr., J. C. Tully, and M. J. Cardillo, J. Chem. Phys. **87**, 6725 (1987).

[50] S. Viti (private communication).

[51] S. Viti, M. P. Collings, J. W. Dever, M. R. S. McCoustra, and D. A. Williams, Mon. Not. Roy. Astron. Soc. **354**, 1141 (2004).